JACS
JOURNAL OF THE AMERICAN CHEMICAL SOCIETY

Article

pubs.acs.org/JACS

Specific Ions Modulate Diffusion Dynamics of Hydration Water on Lipid Membrane Surfaces

Jinsuk Song,[†] John Franck,[∥,†] Philip Pincus,[‡] Mahn Won Kim,[§] and Songi Han*[,†]

[†]Department of Chemistry and Biochemistry and [‡]Materials and Physics Department, University of California, Santa Barbara, Santa Barbara, California 93106, United States

[§]Department of Physics, KAIST, Daejeon 305-701, Republic of Korea

Supporting Information

ABSTRACT: Effects of specific ions on the local translational diffusion of water near large hydrophilic lipid vesicle surfaces were measured by Overhauser dynamic nuclear polarization (ODNP). ODNP relies on an unpaired electron spin-containing probe located at molecular or surface sites to report on the dynamics of water protons within ∼10 Å from the spin probe, which give rise to spectral densities for electron−proton cross-relaxation processes in the 10 GHz regime. This pushes nuclear magnetic resonance relaxometry to more than an order of magnitude higher frequencies than conventionally feasible, permitting the measurement of water moving with picosecond to subnanosecond correlation times. Diffusion of water within ∼10 Å of, i.e., up to ∼3 water layers around the spin probes located on hydrophilic lipid vesicle surfaces is ∼5 times retarded compared to the bulk water translational diffusion. This directly reflects on the activation barrier for surface water diffusion, i.e., how tightly water is bound to the hydrophilic surface and surrounding waters. We find this value to be modulated by the presence of specific ions in solution, with its order following the known Hofmeister series. While a molecular description of how ions affect the hydration structure at the hydrophilic surface remains to be answered, the finding that Hofmeister ions directly modulate the surface water diffusivity implies that the strength of the hydrogen bond network of surface hydration water is directly modulated on hydrophilic surfaces.

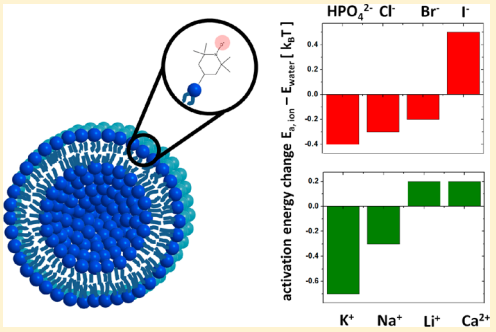

INTRODUCTION

Water is essential in all biological systems, as a solvent medium and as molecular species that modulate global and specific interactions between biomolecular surfaces, where its role in biology is multifaceted, spanning diverse length and time scales. The human body consists of 70% water, and cell membranes and proteins need hydration water for their structural stability and function, such that in many cases the core protein structure and function are not preserved upon dehydration.[1−4] Ions in water play an important role in shielding electrostatic interactions,[5] while some protein function is specifically tuned to the ion type for transport or sensing.[6] Generally, ions are known to modulate macromolecular interaction in water, following the Hofmeister effect or the specific ion effect.[7] As was reported in Hofmeister's original work[8] on proteins, colloids, and oligomers, the order of the ion concentration that induces precipitation versus solubilization is conserved over a large number of biomolecular, protein, and chemical surfaces and is often referred to as the Hofmeister series.

The Hofmeister effect has been observed in many different systems. Sodium phosphate buffer's pH is modulated in the presence of specific anions.[9] The surface tension[10,11] and surface potential[12] of the air−water interface change, and the hydrophobic carbon chain vibrational dynamics of octadecylamine monolayers[13] and the ordering and stability of lipid bilayers[14−16] are also altered, following the Hofmeister series. From the folding, precipitation, and aggregation of macromolecules[17−19] to the kinetics of protein complex formation,[20,21] over a wide range of systems, the ranking following the Hofmeister series is conserved with rare modification.

However, the debate continues as to what the exact molecular mechanism behind the Hofmeister series is. Ion concentration has been shown to increase with the size of monovalent halides[11,22−25] at the air−water interface, but only a few indirect experimental studies report on ion concentrations near lipid bilayers[19,26] and protein surfaces. Ion concentration near phosphocholine lipid bilayers has been studied by molecular dynamics simulation. However, the details of the finding depend on the specific force-field models employed.[27] Still, the general finding is that larger-sized cations adsorb at the bilayer surface less than smaller-sized cations,[28] contrary to the experimental observations that suggest the larger-sized ion to adsorb more readily at the bilayer surface.[19,26]

Ion-induced structural changes of the surrounding waters have been suggested to involve only the first hydration layer around the ion[29,30] and not affect the longer-range or bulk property of water.[31] In the past, ions have also been categorized

Received: December 3, 2013
Published: January 23, 2014

   dx.doi.org/10.1021/ja4121692 | J. Am. Chem. Soc. 2014, 136, 2642−2649

as water structure makers/breakers to rationalize the Hofmeister effect, but recent neutron diffraction experiment and analysis conclude that the number of water molecules involved in the hydration of K^+ and Na^+ are the same,[32] even though these ions present different Hofmeister effects. Thus, the concept of ions generally altering the *bulk* water structure, in the absence of molecular surfaces, does not seem plausible in explaining the effects of ions at the molecular level on surfaces in electrolyte solutions. However, it has been discussed in the literature that the ion's effect on the *local* hydration water structure directly surrounding the ions[29,30,32] can differ depending on the ion type. The pair correlation function between K^+ and the water molecules in its hydration shell is broader with respect to the distance than that of Na^+, and water dipoles in the vicinity of the ion are more disordered for K^+ than Na^+, although the total number of water molecules involved in hydrating the cation is the same.[32] By extension, near macromolecular surfaces, ion density and ion-induced local changes of water structure have been suggested to differ between ions and play key roles. However, it is difficult to detect these properties experimentally under realistic solution conditions and near molecular surfaces. This study reports on the direct experimental observation of changes of the water structure near chemical defects and macromolecular surfaces in the presence of specific ions in dilute solution, by measuring the local diffusion coefficient of 2−3 water layers around the molecular or surfaces sites of interest when various electrolytes are present in the solution at 100 mM concentrations.

Water diffusion is driven by random thermal motion. For a water molecule to move, it has to overcome local binding energy barriers. Without any surface and electrolytes present, at 25 °C, the water diffusion constant is $\sim 2.4 \times 10^{-9}$ m^2/s with an activation energy of 19 kJ/mol.[33] The average number of hydrogen bonds in bulk water is ∼2.4.[34] When molecular or macroscopic surfaces are present, the activation energy for water diffusion nearby is altered, depending on the adsorption energy to the surface and the changes in the hydrogen bonding energy with other water molecules for restructuring. Ions can further alter the hydrogen bond network of water and its adsorption to the surface. Whatever the exact molecular mechanism of this modulation, changes in the local water diffusion directly reflect changes in the local water structure and the interaction energy of water with the surface, whose effect can be quantified as changes in the activation energy for the diffusion of local water near the surface.

In this study, the local translational diffusivity of water near a small chemical defect and a large hydrophilic lipid vesicle surface is reported to change due to the presence of specific ions nearby. The water translational dynamics was quantified with the Overhauser dynamic nuclear polarization (ODNP) relaxometry technique that permits the measurement of water dynamics within ∼10 Å near a spin probe,[35,36] a physical property otherwise experimentally inaccessible under dilute solution conditions, as employed here. Employing ODNP, we find, near chemical defects, water diffusion to be affected by the electrostatic forces between polarized water and nearby ions. However, around hydrophilic lipid vesicle surfaces, water diffusion is found to be more dramatically retarded, due to the attraction of surface water layers to the large hydrophilic surface, whose local water diffusivity is additionally modulated when specific ions are present in solution, with order following the Hofmeister series. Their effects on the local water structure at hydrophilic surfaces will be discussed.

EXPERIMENTAL SECTION

Theory and Method of ODNP Data Analysis. When two types of spins I and S interact through dipolar coupling in a static magnetic field $\mathbf{B}_0$, its total Hamiltonian H can be written as follows[37]

$$-H = \gamma_S \hbar(\vec{S}\cdot\vec{B}_0) + \gamma_I \hbar(\vec{I}\cdot\vec{B}_0) + \gamma_S\gamma_I\hbar^2\left[\frac{3(\vec{I}\cdot\vec{r})(\vec{S}\cdot\vec{r})}{r^5} - \frac{\vec{I}\cdot\vec{S}}{r^3}\right] \quad (1)$$

where γ_S is the gyromagnetic ratio of the electron; γ_I is the gyromagnetic ratio of the proton; and r is the distance between the two spins. In this experiment, S denotes the free electron spin located between the nitrogen and oxygen of the nitroxide spin label as shown in Figure 1(a), and I denotes the proton nuclear spin of the water molecule. The first two terms are the Zeeman terms for the electron spin S and nuclear spin I, and the third term is the dipolar interaction term between spin S and I, which induces exchange of spin states between S and I. Because dipolar interaction is dependent on the distance between the spins, the dynamics of the nuclear spin I relative to the electron spin S affects the rate at which the spin state changes due to their dipolar interaction.

In a static magnetic field of 0.35 T, the electron spin resonance (ESR) of spin S can be saturated when irradiated with microwave fields at ∼9.8 GHz frequencies. The process of saturating the electron spins S can change the polarization of the proton spins I in the presence of dipolar coupling between an S and an I spin, in which continued flips of the S spin magnetic moments driven by microwave irradiation induce flops of the I spin magnetic moments, if the energy for the S spin flip and the I spin flop is matched by the (relative) molecular motion of the I spins. The 658-fold higher initial polarization of the S compared to I spins originates from $\gamma_S/\gamma_I = 658$ as defined earlier. The nature of the dipolar coupling driven S−I cross-relaxation can result in a large and inverted enhancement of the proton NMR signal and changes in the proton's longitudinal relaxation time, whose magnitude sensitively depends on the molecular motion of the I spin with respect to the S spin.

The time evolution of the macroscopic magnetization can be described by the Bloch equation

$$\frac{d\langle I_z\rangle}{dt} = -(w_0 + 2w_1 + w_2 + 2w^0)(\langle I_z\rangle - I_0) - (w_2 - w_0)(\langle S_z\rangle - S_0) \quad (2a)$$

in which w_0 is the transition rate at which spin I and spin S change in opposite direction so that the total spin quantum number change is 0; w_2 is the transition rate at which spin I and spin S change in the same direction so that the total spin quantum number change is 2; and w_1 is the transition rate at which spin I changes its spin state so that the total spin quantum number change is 1. I_0 and S_0 are the equilibrium magnetization of spins I and S in the absence of dipolar coupling, while $\langle I_z\rangle$ and $\langle S_z\rangle$ are the altered magnetization in the presence of dipolar coupling. By rearranging eq 2a, in the steady state, the NMR signal enhancement can be expressed as follows[38]

$$\frac{\langle I_z\rangle}{I_0} = 1 - \frac{w_2 - w_0}{w_0 + 2w_1 + w_2}\frac{w_0 + 2w_1 + w_2}{w_0 + 2w_1 + w_2 + 2w^0}\frac{\langle S_z\rangle - S_0}{I_0} = 1 - \xi\left(1 - \frac{T_1}{T_{10}}\right)s\frac{|\gamma_S|}{\gamma_I} \quad (2b)$$

where s is the total saturation factor of the nitroxide's ESR, which approaches 1 when the spin S is saturated with the microwave power. With the concurrent measurement of the longitudinal relaxation time of the water protons in the presence, $T_1 = 1/(w_2 + 2w_1 + w_2 + 2w^0)$, and in the absence of the of the nitroxide radical spin label, $T_{10} = 1/2w^0$, and by quantifying the NMR signal enhancement, $\langle I_z\rangle/I_0$, the coupling constant $\xi = (w_2 - w_0)/(w_0 + 2w_1 + w_2)$ can be obtained that expresses the difference in the S−I cross-relaxation rates over the sum of all relaxation rates of the I spins induced by the dipolar coupling to the S spins.

dx.doi.org/10.1021/ja4121692 | J. Am. Chem. Soc. 2014, 136, 2642−2649

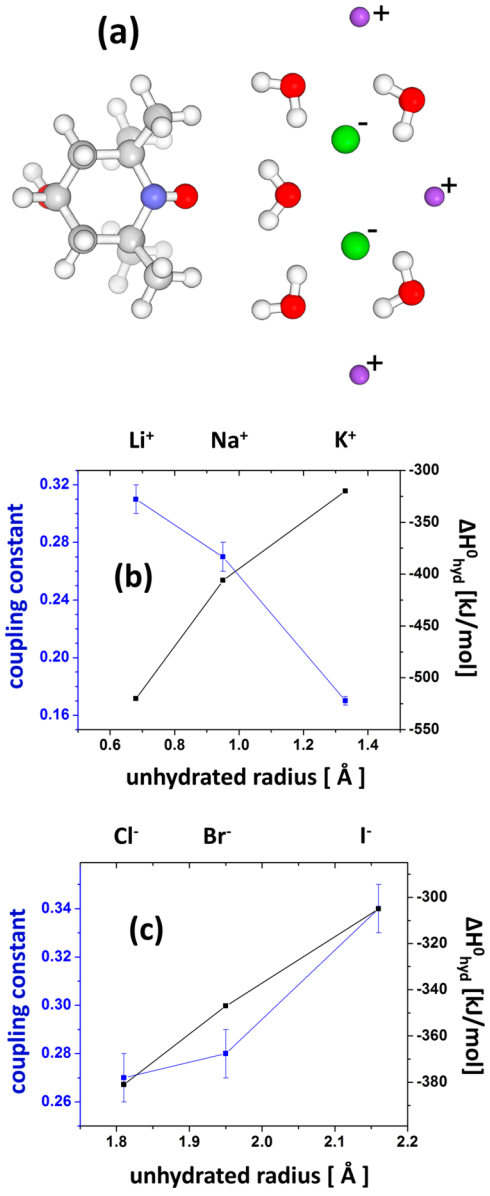

Figure 1. Water diffusion near small chemical defects changes with ion types. (a) Schematic diagram of 4-hydroxy-tempo in electrolyte solution. Oxygens are drawn in red, hydrogen in white, cations in violet, and anions in green. It is not drawn to scale. Hydrogens in water are closer to the nitroxide region of 4-hydroxy-tempo than oxygens in water on average.[46] (b) Coupling constants and hydration enthalpies[43] of various cations were drawn as a function of their unhydrated radius[42] when the anion was fixed as Cl^-. Coupling constants decrease with the unhydrated radius of the cation. Water diffusion near 4-hydroxy-tempo in electrolyte solution is slower with larger-size cations. (c) Coupling constants and hydration enthalpies[43] of various anions were drawn as a function of their unhydrated radius[42] when the cation was fixed as Na^+. Coupling constants increase with the unhydrated radius of the anion. Water diffusion near 4-hydroxy-tempo in electrolyte solution is faster with larger-size anions.

Assuming the dipolar coupling to be the dominant interaction (e.g., no scalar interaction between the S and I spin), the angle between the S and I spins to be isotropically distributed, and the I spin density (i.e., water density) to be constant within ∼10 Å from the S spin (of the spin label), the coupling constant ξ can be written as[38]

$$\xi = \frac{6J(\omega_S + \omega_I) - J(\omega_S - \omega_I)}{6J(\omega_S + \omega_I) + 3J(\omega_I) + J(\omega_S - \omega_I)} \quad (3)$$

with following expression for the spectral density function $J(\omega)$[39]

$$J(\omega) = \frac{8\tau_c}{27b^3}\left[\left(1 + \frac{5}{8}\sqrt{2\omega\tau_c} + \frac{1}{4}\omega\tau_c\right) \Big/ \left(1 + \sqrt{2\omega\tau_c} + (\omega\tau_c) + \frac{1}{3}\sqrt{2}(\omega\tau_c)^{3/2} + \frac{16}{81}(\omega\tau_c)^2 + \frac{4}{81}\sqrt{2}(\omega\tau_c)^{5/2} + \frac{1}{81}(\omega\tau_c)^3\right)\right] \quad (4)$$

where ω_S and ω_I are the Larmor frequencies of the electron and proton nuclear spin, respectively. b is the closest distance between the spin S and spin I. This spectral density is valid when the diffusion of the I spin relative to the S spin dominates the relaxation process. It was experimentally shown by field cycling relaxometry that diffusion is the major relaxation mechanism for nitroxide radicals in aqueous solution[35] and for covalently bound nitroxide radical probes at the lipid headgroup of POPC lipid bilayer vesicles.[40] This is mainly because the Larmor frequencies for the spin label S and the ^1H nuclear spin I are largely decoupled (9.8 GHz for the S spins vs 14.8 MHz for the I spins), and relaxation time for the electron spin S in the order of microseconds is much larger compared to the subnanosecond diffusion correlation time τ_c.

The diffusion correlation time τ_c is chosen as the time it takes for the diffusing water to move a distance b, the closest distance between the spin S and spin I, while the dipolar coupling is effective between the spin label electron and water proton and is expressed as[41]

$$\tau_c = \frac{b^2}{D_w} \quad (5)$$

where D_w is the diffusion coefficient of the I spin-bearing atom (here water) near the S spin (here the spin label) within the distance b, assuming the diffusion coefficient of the spin label is negligible compared to that of the surrounding waters. For the analysis in this study, we employed an empirically determined value for the distance of closest approach of b = 3.5 Å.

Materials. 4-Hydroxy-tempo (free radical, Aldrich, 176141), POPC (1-palmitoyl-2-oleyl-*sn*-glycero-3-phosphocholine, Avanti, 850457), and spin-labeled POPC (1-palmitoyl-2-oleyl-*sn*-glycero-3-phospho-(tempo)choline, Avanti, 810609) were used without further purification. Sodium chloride (Fisher, S271), sodium bromide (Sigma, 71329), sodium iodide (Sigma, 383112), sodium phosphate monobasic (J. T. Baker, 4062-01), sodium phosphate dibasic (Fisher, S369), lithium chloride (Sigma, L4408), potassium chloride (Fisher, P217), ammonium chloride (Fisher, A661), and calcium chloride (Sigma, 223506) were dissolved in deionized (18.2 MΩ) water to obtain 100 mM electrolyte solutions.

Lipid Vesicle Sample Preparation Method. POPC was dissolved in chloroform to 25 mg/mL (∼33 mM) concentration. An amount of 100 μL of the POPC solution was spread in a round-bottom glass tube. The sample was dried under N_2 gas for 15−20 min and further vacuum-dried overnight to obtain the lipid film. After adding 100 μL of deionized water or appropriate electrolyte solution, it was stored at room temperature for 2.5 h. The solution was vortexed frequently to get even distribution of the lipid film across the aqueous solution. Then, the lipid solution was extruded with a mini-extruder (Avanti, 610000) to get large unilamellar vesicles (LUVs) with ∼200 nm diameters. The vesicle size was checked with a dynamic light scattering (DLS) instrument (Malvern, ZEN3600). Surface spin labeled POPC vesicles were prepared by mixing 2 mol % (∼650 μM) of nitroxide spin labels covalently attached to the PC's choline group with the POPC lipid solution in chloroform before the drying process. The DLS measurements show that the average vesicle sizes range between 170 and 200 nm for all samples prepared in various electrolyte solutions used in the experiments. The vesicle size difference with and without spin-labeled POPC lipids is less than 10%.

dx.doi.org/10.1021/ja4121692 | J. Am. Chem. Soc. 2014, 136, 2642−2649

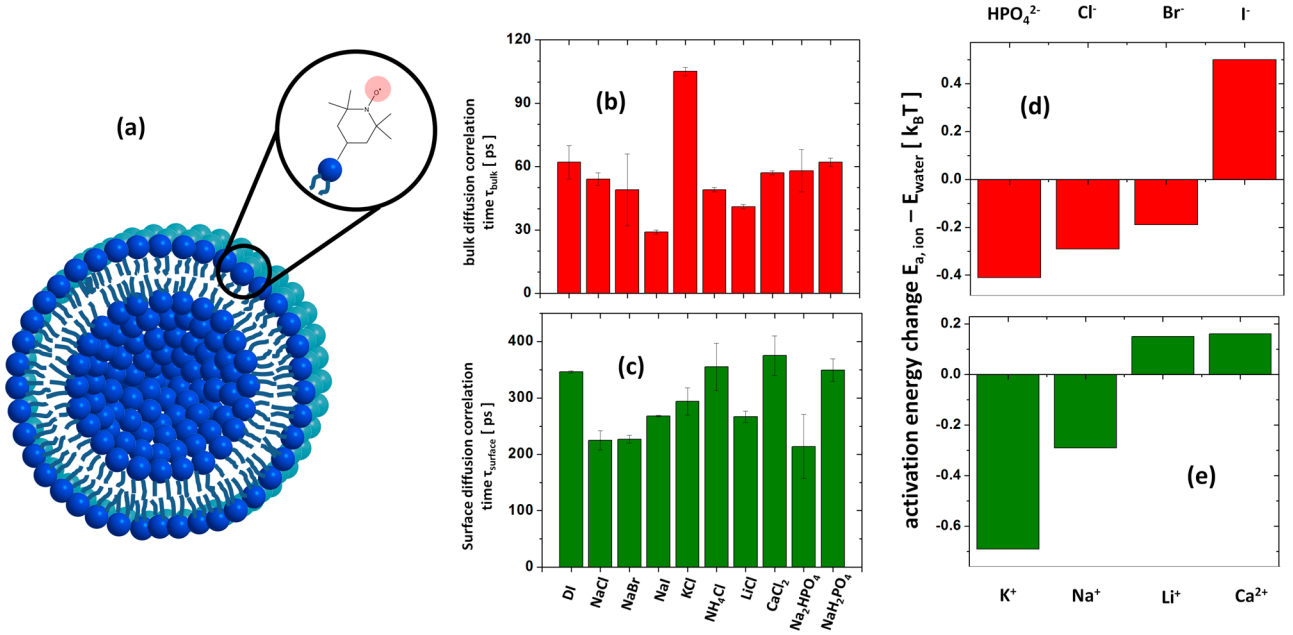

Figure 2. Ion affects water diffusion near the unilamellar vesicle surface with the order of Hofmeister series. (a) Schematic diagram of spin-labeled phospholipid vesicles in electrolyte solution. Spin-label, tempo, was drawn in skeletal formula. It is not drawn to scale. (b) Bulk diffusion correlation time of water near 4-hydroxy-tempo, calculated from eqs 3 and 4, is presented in various 100 mM electrolyte solutions. Electrolyte types are indicated at the bottom of part (c). Diffusion correlation time is inversely proportional to diffusion constant. (c) Surface diffusion correlation time of water near ∼200 nm phospholipid vesicle surfaces, calculated from eqs 3 and 4, is presented in various 100 mM electrolyte solutions. Electrolyte types were indicated at the bottom of the graph. (d) Water diffusion activation energy, calculated from eq 7 with bulk and surface diffusion correlation times, is presented for anions. It follows Hofmeister series. (e) Water diffusion activation energy, calculated from eq 7, with bulk and surface diffusion correlation times, is presented for cations. It follows Hofmeister series. Activation energy error is $\pm 0.1 k_B T$.

RESULTS AND DISCUSSION

Water Diffusion near Small Chemical Defects. Local water dynamics near the nitroxide radical spin probe, 4-hydroxy-tempo, which is a small molecule with volume significantly smaller than 1 nm^3 and here considered as a small chemical defect, was measured in bulk water solution that contained otherwise no molecular surfaces (illustrated in Figure 1(a)). The concentration of 4-hydroxy-tempo was chosen to be 650 μM. The coupling constant, calculated from eq 2b, of water near the radical probe 4-hydroxy-tempo in deionized water is measured to be $\xi = 0.25 \pm 0.03$. A complete list of the coupling constants of various 100 mM electrolyte solutions is presented in the Supporting Information. The larger the coupling constant, the smaller the diffusion correlation time, and the faster the water diffusion, as expressed in eqs 3, 4, and 5. Some electrolytes cause water to diffuse faster around the 4-hydroxy-tempo radical probe than in deionized water, such as NaI that changes the bulk water coupling constant to 0.34 ± 0.01, while other electrolytes such as KCl change the bulk water coupling constant to 0.17 ± 0.003, thus exerting the opposite effect.

Figure 1(b) and (c) presents the effects of cation (b) and anion (c) for monatomic electrolytes, with both data presented as a function of the unhydrated ion radius.[42] Figure 1(b) presents the changes in the coupling constant with varying cation type, while fixing the counteranion as Cl^-. Figure 1(c) presents the coupling constant change with varying anion type, while fixing the countercation as Na^+. These results illustrate the known relationship between the unhydrated ion radius and the enthalpy of hydration,[43] which decreases with the ion radius for both cations and anions. As the cation radius increases, the coupling constant decreases; i.e., water near the 4-hydroxy-tempo label in the electrolyte solution diffuses slower. In contrast, when the anion radius increases, the coupling constant increases; i.e., water near the 4-hydroxy-tempo label in the electrolyte solution diffuses faster. The observation of clearly opposite effects exerted by the cations versus the anions on the coupling constant measured through the chemical defect suggests that the water diffusion around the chemical defects is modulated by the electrostatic interaction with nearby ions. Here, we first present the measurement of the coupling constant, as it is an experimentally determined, model-free parameter, while the extracted diffusion correlation time for local water is model-dependent, as expressed with eq 4. Nonetheless, the diffusion correlation time has a broadly understood physical meaning that allows comparisons to results from other techniques or computational studies and thus will be presented in Figure 2. Figure 2(b) shows the diffusion correlation time τ_{bulk} of water calculated from the coupling constants (ξ) following eqs 3 and 4. We denote it as the *bulk water* diffusion correlation time because it captures the water diffusivity in bulk solutions in the presence of electrolytes but in the absence of other, here lipid vesicle, surfaces.

The ESR spectral linewidth and the hyperfine coupling tensor, **A**, of the 4-hydroxy-tempo radical probe are sensitive to changes in the local electric field and the rotational motion of the radical, given the sensitivity of the Zeeman and hyperfine interaction of the nitroxide electron spin with respect to the main and local magnetic fields.[44] The ion mass and size are comparable to the radical mass and size, so that direct adsorption of ions to the radical probe with ∼100 ps lifetime or longer should change the rotational motion of the complex, which would be reflected in changes of the ESR lineshape, as eluded to above. Also, the charges of adsorbed ions can change the hyperfine coupling of the radical probe that is sensitive to

dx.doi.org/10.1021/ja4121692 | J. Am. Chem. Soc. 2014, 136, 2642−2649

the local dielectric constant. The hyperfine splitting constant, A_{zz}, has been found to correlate with the local polarity near the spin probe, when its motion is immobilized surveying protein and lipid membrane surfaces.[44,45] Notably, under the here studied experimental conditions, the ESR spectrum is observed to remain unaltered with the electrolyte species and electrolyte concentration in solution (see Supporting Information), suggesting that there is no direct adsorption of ions to the spin label. The water molecules in the first hydration layer of 4-hydroxy-tempo, in the absence of ions, prefer an orientation where the hydrogen of water in the first hydration layer is closer to the nitroxide moiety than the oxygen of water because the nitroxide moiety of the 4-hydroxy-tempo radical is electron-rich.[46] When an ion comes nearby the first hydration layer of 4-hydroxy-tempo, the ion competes with 4-hydroxy-tempo for taking up the water molecule of the hydration layer. Cations that have been confirmed by ESR to not directly or closely bind to 4-hydroxy-tempo, but reside outside the first hydration layer of 4-hydroxy-tempo nearby, then attract the oxygen of the water molecules and tend to pull on the water of the 4-hydroxy-tempo hydration layer, while anions repel the water oxygen of the 4-hydroxy-tempo hydration layer via electrostatic interaction. When the anion is fixed as Cl^-, as the countercation size increases and thus its charge density decreases, the strength of the countercation's pulling force for water oxygen decreases. As a result, water is more closely attracted to, and can less freely diffuse away from, the 4-hydroxy-tempo probe. The cation and anion exert the opposite effect and work cooperatively, so that for the case of NaCl the diffusion of hydration water of 4-hydroxy-tempo is similar to the diffusion of bulk water in the absence of electrolytes. When the anion is fixed, as the cation size increases from $Li^+ < Na^+ < K^+$, the cation attracts water less strongly, as reflected in the hydration enthalpy in Figure 1(b). The diffusion of the hydration water of 4-hydroxy-tempo decreases with this order, and the opposite is true for the anion when the cation is fixed as Na^+ in Figure 1(c). As shown in Figure 1(b) and (c), the relative change in the coupling constant is correlated with the relative changes in the hydration enthalpy that originate from the changes in charge density, given the size of the ion,[42] while they rank in opposite order for cations versus anions, given their opposite charges.

The pulling/pushing force is only predominantly effective for the first hydration layer of 4-hydroxy-tempo, because water (in the hydration layer of 4-hydroxy-tempo and bulk water) experiences fast reorientation dynamics, so that the distance from the water proton to the nitroxide and the water oxygen to the nitroxide is, on average, equal for water more than one hydration shell away from the nitroxide. In addition, the efficiency of the dipolar coupling decays with 1/distance^6 from the nitroxide moiety.

Not only the unhydrated ion but also the hydrated ion combined with its hydration layer can compete with 4-hydroxy-tempo for taking up a water molecule of the 4-hydroxy-tempo hydration layer. This effect will be smaller, in general, than the effect of the unhydrated ion. It is thought that ion-induced structural changes of the surrounding waters only involve the first hydration layer around the ion.[29,30] This suggests that the interaction between water in the first hydration shell and water outside the first hydration shell of the ion is not much different from the water−water interaction in bulk water, in the absence of ions. Thus, the effect of hydrated ions on the diffusion of 4-hydroxy-tempo's hydration water will be less significant. For this reason, the coupling constant for water diffusion is plotted against the ion's unhydrated radius in Figure 1(b) and (c).

Gao et al. proposed that cations can polarize its hydration water molecules to make them strong hydrogen bond donors.[47] For the donor hydrogen of the ion's hydration shell, its strength as a hydrogen bond donor decreases with increasing cation size, given the cation's decreasing charge density. Thus, the pulling force of the *donor hydrogen* of the ion's hydration shell on the *acceptor oxygen* of the first hydration layer of 4-hydroxy-tempo will also decrease with increasing cation size. This is consistent with the experimental results presented in this study. However, unlike in Gao et al.'s system, where polypeptides display strong hydrogen bond sites,[47] the electron in the nitroxide moiety of the spin labels is delocalized over the nitrogen and oxygen, so that it does not serve as a strong hydrogen bond acceptor but rather displays a dynamic hydrogen bond structure.[46] Also, water in the first hydration layer of 4-hydroxy-tempo diffuses away fast and is replaced by other water molecules, where the probability of strongly polarized hydration water of the cation to reside at the nitroxide site is ∼100 times smaller than for unperturbed water at 100 mM electrolyte concentration. In addition, strongly bound water to 4-hydroxy-tempo, if at all, contributes less effectively to the coupling constant presented in eq 3, given its slower dynamics relative to the ODNP resonance frequency. Judging by the experimentally measured water diffusion constant near 4-hydroxy-tempo, which decreases less than 2 times compared to bulk water, and in the presence of Li^+ and with most of the anions even increases, it can be concluded that the role of strongly polarized hydration water of the cation near the nitroxide moiety is negligible. Still, the hydrogen of the cation's hydration water is sufficiently polarized to compete with 4-hydroxy-tempo for pulling on the 4-hydroxy-tempo's hydration water. If the Overhauser dynamic nuclear polarization scheme could be applied directly to magnetically active ions (e.g., ^{7}Li or ^{23}Na), which is currently not feasible given technical challenges, it would be very interesting to observe the relationship of the ion hydration water diffusion and the Stokes radius of the ion in the future.

Water Diffusion near Large Hydrophilic Vesicle Surfaces. Figure 2(a) schematically presents the measurement of local water dynamics near the lipid vesicle surface, whose hydrodynamic radius is ∼200 nm. The spin-labeled lipid molecule (PC-TEMPO) displays a nitroxide radical probe at the terminus of the hydrophilic lipid headgroup, off the quarternary ammonium of the choline moiety, while its hydrophobic tail is identical to that of the unlabeled POPC lipid molecule. The coupling constant of surface water on POPC lipid vesicles dispersed in deionized water measured through the PC-TEMPO probe at a distance more than 5 Å away from the phosphate group level was found to be 0.042 ± 0.001. A complete list of the measured coupling constants between the spin label and the water near the POPC lipid vesicle surfaces in various electrolyte solutions at 100 mM concentrations is presented in the Supporting Information. The coupling constant of 0.042 ± 0.001 found for surface water near the POPC lipid vesicle surfaces, in the absence of electrolytes, translates into a diffusion correlation time, $\tau_{surface}$, of 346 ± 7 ps (according to eqs 3 and 4), whose value is in agreement with the 335 ps values measured with field cycling relaxometry before.[40] This corresponds to a ∼5-fold retardation from the bulk water diffusion value of 62 ± 8 ps, consistent with previous reports on hydration water dynamics on the phospholipid membrane[48] and hemoglobin[49] surfaces. Thus, the surface

water diffusivity on lipid vesicles is slowed down significantly compared to that of bulk water, while it is decoupled from the motion of the phospholipid molecules whose lateral diffusion constant is $\sim 1.8 \times 10^{-12}$ m^2/s, i.e., ~2 orders of magnitude smaller than that of water.[50] The observation of surface water retardation is also in accordance with non-NMR-based experimental and theoretical studies that found water in the hydration layer near hydrophilic interfaces to present higher density[51−54] and slower rotational as well as translational motion.[55] This is consistent with the fairly hydrophilic surface of the phosphocholine lipid headgroup attracting and binding water molecules[56] and thus significantly slowing down the translational motion of water within the surface hydration layer.

Figure 2(c) presents the diffusion correlation time $\tau_{surface}$ calculated from the coupling constant values using eqs 3 and 4. It was denoted as the *surface diffusion* correlation time, as it averages over the diffusion of water near (~10 Å) the vesicle surface and in fact is dominated by the surface characteristics of attracting hydration water. Notably, nearly all electrolytes were found to enhance the surface water diffusivity compared to that in deionized water, although there are a few exceptions. This is in contrast to the characteristics of *bulk diffusion* correlation time of water measured near (~10 Å) the chemical defect, the 4-hydroxy-tempo probe, in solution that is free of molecular surfaces and thus is not affected by the surface characteristics.

The activation energy for water diffusion can be expressed by the Arrhenius equation as[33,40]

$$D_{surface} = A \cdot e^{-E_{surface}/k_B T} \text{ and } D_{bulk} = A \cdot e^{-E_{bulk}/k_B T} \quad (6a)$$

where $D_{surface}$ is the water diffusion constant near the vesicle surface and D_{bulk} is the bulk water diffusion constant in the absence of the vesicle surface. The change in the activation energy in water without and with ions, $\Delta E_{water/ion} = E_{surface} - E_{bulk}$, can then be calculated as follows

$$\begin{aligned} D_{surface}/D_{bulk} &= \tau_{bulk}/\tau_{surface} \\ &= e^{-(E_{surface}-E_{bulk})/k_B T} \\ &= e^{-\Delta E_{water/ion}/k_B T} \end{aligned} \quad (6b)$$

Here, τ_{bulk} and $\tau_{surface}$ are the bulk water and POPC surface diffusion correlation time, respectively, where eq 5 was used to replace the diffusion constant with the diffusion correlation time, or vice versa.

The value for ΔE_{water} determined in this study from surface diffusion correlation time on POPC vesicles in the absence of electrolytes, $\tau_{surface,water}$, and bulk water diffusion correlation time near 4-hydroxy-tempo probes, $\tau_{bulk,water}$, is $1.7k_BT$, which is within an error of $\Delta E_{water} = 1.6k_BT$ as was previously determined for POPC vesicle surfaces by means of field cycling NMR relaxometry measurements with temperature variations[40] and the known bulk water activation energy.[33,40]

As we can assume the relation eqs 6a and 6b to be valid for 100 mM aqueous electrolyte solutions, the change in activation energy for water diffusion in the presence of ions, $\Delta E_{ion} - \Delta E_{water}$, can be calculated as

$$\begin{aligned} &\frac{D_{surface,ion}}{D_{surface,water}} \cdot \frac{D_{bulk,water}}{D_{bulk,ion}} \\ &= \frac{\tau_{surface,water}}{\tau_{surface,ion}} \cdot \frac{\tau_{bulk,ion}}{\tau_{bulk,water}} \\ &= e^{-(\Delta E_{ion}-\Delta E_{water})/k_B T} \end{aligned} \quad (7)$$

using bulk and surface diffusion coefficients or bulk and surface diffusion correlation times, as presented in Figures 2(b) and (c). Here, the subscript, ion, indicates the presence of the electrolytes.

Figures 2(d) and (e) present this change in the value for the activation energy, $\Delta E_{ion} - \Delta E_{water}$, separately for the cations and anions. A complete list of activation energies of surface water diffusion in various 100 mM electrolyte solutions is presented in the Supporting Information. Because these values are corrected for the effects from the 4-hydroxy-tempo probes that act as chemical defects, the variations solely originate from the effect of electrolytes exerted on the surface water diffusion on POPC lipid vesicle surfaces. Their order follows the Hofmeister series,[7,8] as presented in Figures 2(d) and (e). For all 100 mM electrolyte solutions tested in this study, notably the *change* in the surface diffusion activation energy is less than $1k_BT$. The change in activation energy for diffusion is positive (higher energy barrier for surface water diffusion) in the presence of larger anions such as I^- and smaller cations, while it is negative (lower energy barrier for surface water diffusion) in the presence of smaller anions and larger cations such as K^+.

Regardless of the sign of the charge, the ions that are ranked high in the Hofmeister series, such as HPO_4^{2-} and K^+ known to induce salting out of macromolecules at high electrolyte concentration, also show negative change in the diffusion activation energy near the hydrophilic surfaces, even at lower concentration than what induces aggregation of macromolecules. It is carefully checked that the vesicles are well dispersed in various 100 mM electrolyte solutions, so the signature of greater disturbed hydration water structure and lowered activation energy for the diffusion of surface hydration water is not affected by intervesicle interactions. Given that salting out or aggregation is a consequence of the macromolecules preferring interaction with its own or neighboring macromolecular chains over the interaction with the surrounding water, it is reasonable that surface water under these conditions would show enhanced diffusivity and smaller activation energy barrier for diffusion, i.e., experience weaker interaction with the surface and nearby water molecules. Conversely, Hofmeister ions that tend to dissolve or unfold a macromolecule in water yield higher activation energy barrier for surface water diffusion, as the water is more attracted to the surface and nearby surface water. The NH_4^+ ion is a notable exception, which may be an artifact caused by the proton NMR signal of the ammonium ion. In the relatively low magnetic field employed in this experiment, the water and ammonium proton NMR signal cannot be distinguished, so that their relaxation processes may interfere. The diffusion activation energy change for surface hydration water in the presence of LiCl and $CaCl_2$ electrolytes is indistinguishable. However, it may be a coincidence, where these ions no longer exert the same effects on surface water diffusion near other macromolecular surfaces.

Around hydrophilic surfaces, water molecules in the hydration layer can form a dense hydrogen bond network,[57] which plays an important role in building up electrochemical potentials at active sites of HiPIP or Ferredoxn,[1] and also otherwise affect the bioactivity of proteins.[2] Local ordering of the water network, the residence time,[58] and reorientation dynamics[59] of water at hydrophilic sites or surfaces depend not only on their overall hydrophilicity but also on the specific chemical structure, polarity, and topology of the surface.[53,60,61] Although ions are found not to change the hydrogen bond network in bulk water further away than one hydration

dx.doi.org/10.1021/ja4121692 | J. Am. Chem. Soc. 2014, 136, 2642−2649

layer[29−32] around the individual ions, they can disrupt the hydrogen bond network of water near macromolecular surfaces with longer ranging effects.[61] Fundamentally, this suggests that the hydrogen bond network near macromolecular, hydrophilic surfaces is different from that of bulk water, in that the isotropy of the network is broken by the surface by its strong attraction of surface water. Our observation of modulation in water diffusion on surfaces in the presence of ions is consistent with this concept that specific ions interfere with the interaction between the water and the molecular surface.

Implication of Specific Ion Effects on the Water Diffusion near Hydrophilic Surfaces. To what extent and how, at the molecular level, the existing hydrogen bond network in a hydrophilic hydration layer is perturbed by specific ions is not a simple question to answer. It can depend on the existing hydration structure and the individual ion's geometry such as size and charge distribution, as well as its local concentration[19,26,62] at the surface that may differ from the bulk concentration. Many factors affect the individual ion's ability to disrupt the hydrogen bond network near a surface, such as the hydration enthalpy,[43] the sign of charge, and the hydrated or the unhydrated ion radius,[42] depending on whether individual ions lose its hydration water at the surface or not.

In particular, the local ion density at the surface and their density profile are important to better understand the ion's effect on the surface hydration structure and water diffusion but are difficult to experimentally access. Ion concentration at the surface can vary from ion to ion.[19,26,62] Generally, the relative position of the Gibbs dividing surface of an ion[11,63] to water oxygen and hydrogen affects the interaction between the ion and water, as found for bulk water diffusion near the 4-hydroxy-tempo molecule acting as a chemical defect, and will be the case also on macromolecular surfaces. In addition, water diffusion parallel vs perpendicular to the surface can be different,[51] and there can be a specific length scale from the surface across which the water diffusion coefficient relaxes to the bulk water value.[64,65] Although the measured diffusion correlation time in this experiment is averaged over all directions and across approximately 10 Å distances around the spin probe, this level of surface specificity for capturing water diffusion near chemical defects or surfaces in solution, under biologically relevant electrolyte concentrations for the purpose of quantifying the effects of specific ions on the local hydration water structure, is unprecedented.

Notably, ions can alter the phase of the lipid bilayers[16] and the interaction between lipid layers, as reflected in changes in the distance between multilamellar bilayers with the ion type and concentration.[15,66] This observation has been explained by changes in ion-induced van der Waals forces[62,66] and electrostatic forces based on the Debye−Huckel theory.[5] Interestingly, both the changes in the water diffusion activation energy near the hydrophilic vesicle surfaces as observed in this study and the changes reported in the interbilayer distance[15,66] follow the Hofmeister series. Thus, it makes sense to assume that the same molecular mechanism of specific ion effects on surface water diffusivity may underlie the experimental observations of specific ion effects on macromolecular interaction and forces.

It is clear from this study that the changes in the hydration water structure induced by the specific ions result in the modulation of surface hydration water diffusion. The question that this study highlights is whether the modulation of hydration water dynamics directly and predominantly contributes to the modulation of forces between bilayers, in addition to van der Waals and electrostatic interactions that have been found to be directly modulated by specific ions.

■ CONCLUSION

The effect of specific ions on the translational diffusion of water near small chemical defects and around large hydrophilic lipid vesicle surfaces was investigated by the ODNP relaxometry technique. Near 4-hydroxy-tempo spin probes whose volume is <1 nm^3, water diffusion is modulated to be faster or slower according to the ion's pushing or pulling force of the first hydration water molecules near the nitroxide moeity, given the slightly preferential electrostatic interactions between the ion and these neighboring water molecules' oxygen, and found to scale with the sign and density of the ion. Near (∼10 Å) the surface of unilamellar lipid vesicles of 200 nm diameter suspended in solution, specific ions in solution are found to further alter the activation energy for surface water diffusion by modulating the water hydrogen bond network within the surface hydration layer. The order of the observed change in activation energy follows the Hofmeister series. Whether the local ion concentration at the vesicle surface varies with ion types, whether it is different from the global concentration in the bulk solvent, and what the exact molecular mechanism is for the specific ions to change the hydration water structure near surfaces remain open questions. What is clear, however, is that the specific ions that tend to aggregate or precipitate a macromolecule enhance the surface water diffusivity, and the ions that tend to solubilize or unfold a macromolecule lower the surface water diffusivity around hydrophilic surfaces. This suggests that the origin of the Hofmeister ions may be the balancing between macromolecule−water and macromolecule−macromolecule interaction through the modulation of the effective surface hydrophilicity and hydrophobicity mediated by specific ions in dilute solution.

■ ASSOCIATED CONTENT

Supporting Information

Supporting Table S1 and Figures S1 and S2. This material is available free of charge via the Internet at http://pubs.acs.org.

■ AUTHOR INFORMATION

Corresponding Author

songi@chem.ucsb.edu

Present Address

[‖]Department of Chemisty and Chemical Biology, Cornell University, Ithaca, NY 14853.

Notes

The authors declare no competing financial interest.

■ ACKNOWLEDGMENTS

This research was supported by the 2011 NIH Directors New Innovator Award and WCU program through NRF of Korea funded by MEST (R33-2008-000-10163-0). Authors made use of the Materials Research Laboratory Central Facilities supported by the National Science Foundation through the Materials Research Science and Engineering Centers under grant No. DMR 1121053. The MRL is a member of the NSF-funded Materials Research Facilities Network (www.mrfn.org).

REFERENCES

(1) Dey, A.; Jenney, F. E., Jr.; Adams, M. W. W.; Babini, E.; Takahashi, Y.; Fukuyama, K.; Hodgson, K. O.; Hedman, B.; Solomon, E. I. *Science* **2007**, *318*, 1464−1468.
(2) Brovchenko, I.; Oleinikova, A. *Chem. Phys. Chem.* **2008**, *9*, 2695−2702.
(3) Nakagawa, H.; Yoti, J.; Kitao, A.; Kataoka, M. *Biophys. J.* **2010**, *95*, 2916−2923.
(4) Fernandez, A.; Scheraga, H. A. *Proc. Natl. Acad. Sci. U.S.A.* **2003**, *100*, 113−118.
(5) Onsager, L.; Samaras, N. N. T. *J. Chem. Phys.* **1934**, *2*, 528−536.
(6) Choe, S. *Nat. Rev. Neurosci.* **2002**, *3*, 115−121.
(7) Kunz, W., Ed. *Specific Ion Effects*; World Scientific: Singapore, 2010; pp 3−54.
(8) Hofmeister, F. *Arch. Exp. Pathol. Pharmakol.* **1888**, *24*, 247−260.
(9) Salis, A.; Pinna, M. C.; Bilanicova, D.; Monduzzi, M.; Nostro, P. L.; Ninham, B. W. *J. Phys. Chem. B* **2006**, *110*, 2949−2956.
(10) Pegram, L. M.; Record, M. T., Jr. *J. Phys. Chem. B* **2007**, *111*, 5411−5417.
(11) Song, J.; Kim, M. W. *J. Phys. Chem. B* **2011**, *115*, 1856−1862.
(12) Randles, J. E. R. *Phys. Chem. Liq.* **1977**, *7*, 107−179.
(13) Gurau, M. C.; Lim, S. M.; Castellana, E. T.; Albertorio, F.; Kataoka, S.; Cremer, P. S. *J. Am. Chem. Soc.* **2004**, *126*, 10522−10523.
(14) Sachs, J. N.; Woolf, T. B. *J. Am. Chem. Soc.* **2003**, *125*, 8742−8743.
(15) Pabst, G.; Hodzic, A.; Strancar, J.; Danner, S.; Rappolt, M.; Laggner, P. *Biophys. J.* **2007**, *93*, 2688−2696.
(16) Sanderson, P. W.; Lis, L. J.; Quinn, P. J.; Williams, W. P. *Biochim. Biophys. Acta* **1991**, *1067*, 43−50.
(17) Zhang, Y.; Furyk, S.; Bergbreiter, D. E.; Cremer, P. S. *J. Am. Chem. Soc.* **2005**, *127*, 14505−14510.
(18) Leontidis, E. *Curr. Opin. Colloid Interface Sci.* **2002**, *7*, 81−91.
(19) Ivanov, I. V.; Slavchov, R. I.; Basheva, E. S.; Sidzhakova, D.; Karakashev, S. I. *Adv. Colloid Interface Sci.* **2011**, *168*, 93−104.
(20) von Hippel, P. H.; Wong, K. Y. *Biochemisty* **1962**, *1*, 664−674.
(21) Yeh, V.; Broering, J. M.; Romanyuk, A.; Chen, B.; Chernoff, Y. O.; Bommarius, A. S. *Protein Sci.* **2010**, *19*, 47−56.
(22) Ghosal, S.; Hemminger, J. C.; Mun, B. S.; Hebenstreit, E. L. D.; Ketteler, G.; Ogletree, D. F.; Requejo, F. G.; Salmeron, M. *Science* **2008**, *307*, 563−566.
(23) Jungwirth, P.; Tobias, D. J. *J. Phys. Chem. B* **2001**, *105*, 10468−10472.
(24) Levin, Y. *Phys. Rev. Lett.* **2009**, *102*, 147803.
(25) Padmanabhan, V.; Daillant, J.; Belloni, L.; Mora, S.; Alba, M.; Konovalov, O. *Phys. Rev. Lett.* **2007**, *99*, 086105.
(26) Petrache, H. I.; Kimchi, I.; Harries, D.; Parsegian, V. A. *J. Am. Chem. Soc.* **2005**, *127*, 11546−11547.
(27) Gurtovenko, A. A.; Vattulainen, I. *J. Phys. Chem. B* **2008**, *112*, 1953−1962.
(28) Jurkiewicz, P.; Cwiklik, L.; Vojtiskova, A.; Jungwirth, P.; Hof, M. *Biochim. Biophys. Acta* **2012**, *1818*, 609−616.
(29) Omta, A. W.; Kropman, M. F.; Woutersen, S.; Bakker, H. J. *Science* **2003**, *301*, 347−349.
(30) Smith, J. D.; Saykally, R. J.; Geissler, P. L. *J. Am. Chem. Soc.* **2007**, *129*, 13847−13856.
(31) Zhang, Y.; Cremer, P. S. *Curr. Opin. Colloid Interface Sci.* **2006**, *10*, 658−663.
(32) Mancinelli, R.; Botti, A.; Bruni, F.; Ricci, M. A.; Soper, A. K. *J. Phys. Chem. B* **2007**, *111*, 13570−13577.
(33) Wang, J. H.; Robinson, C. V.; Edelman, I. S. *J. Am. Chem. Soc.* **1953**, *75*, 466−470.
(34) Zielkiewicz, Y. *J. Chem. Phys.* **2005**, *123*, 104501.
(35) Armstrong, B. D.; Han, S. *J. Am. Chem. Soc.* **2009**, *131*, 4641−4647.
(36) Overhauser, A. *Phys. Rev.* **1953**, *92*, 411−415.
(37) Solomon, I. *Phys. Rev.* **1955**, *99*, 559−566.
(38) Hausser, K. H.; Stehlik, D. *Adv. Magn. Reson.* **1968**, *127*, 79−139.
(39) Freed, J. H. *J. Chem. Phys.* **1978**, *68*, 4034−4037.
(40) Hodges, M. W.; Cafiso, D. S.; Polnaszek, C. F.; Lester, C. C.; Bryant, R. G. *Biophys. J.* **1997**, *73*, 2575−2579.
(41) Abragam, A., Ed. *Principles of Nuclear Magnetism*; Oxford University Press: London, U. K., 1961; pp 264−305.
(42) Israelachvili, J. N., Ed. *Intermolecular and Surface Forces*; Academic Press: San Diego, United States, 1992; pp 110.
(43) Smith, D. W. *J. Chem. Educ.* **1977**, *54*, 540−542.
(44) Bordignon, E.; Steinoff, H.-J. Membrane Protein Sturcture and Studied by Site-Directed Spin-Labeling ESR. In *ESR Spectroscopy in Membrane Biophysics*; Hemminga, M. A., Berliner, L. J., Ed.; Springer: New York, United States, 2007; pp 129−164.
(45) Marsh, D. *Proc. Natl. Acad. Sci. U.S.A.* **2001**, *98*, 7777−7782.
(46) Armstrong, B. D.; Soto, P.; Shea, J. E.; Han, S. *J. Magn. Reson.* **2009**, *200*, 137−141.
(47) Xie, W. J.; Gao, Y. Q. *J. Phys. Chem. Lett.* **2013**, *4*, 4247−4252.
(48) Franck, J. M.; Scott, J. A.; Han, S. *J. Am. Chem. Soc.* **2013**, *135*, 4175−4178.
(49) Steinhoff, H. J.; Kramm, B.; Hess, G.; Owerdieck, C.; Redhardt, A. *Biophys. J.* **1993**, *65*, 1486−1495.
(50) Devaux, P.; McConnell, H. M. *J. Am. Chem. Soc.* **1972**, *94*, 4475−4481.
(51) Smith, J. C.; Merzel, F.; Verma, C. S.; Fischer, S. *J. Mol. Liq.* **2002**, *101*, 27−33.
(52) Lee, S. H.; Rossky, P. J. *J. Chem. Phys.* **1994**, *100*, 3334−3345.
(53) Giovambattista, N.; Debenetti, P. G.; Rossky, P. J. *Proc. Natl. Acad. Sci. U.S.A.* **2009**, *106*, 15181−15185.
(54) Gallo, P.; Ricci, M. A.; Rovere, M. *J. Chem. Phys.* **2002**, *116*, 342−346.
(55) Zhong, D.; Pal, S. K.; Zewail, A. H. *Chem. Phys. Lett.* **2011**, *503*, 1−11.
(56) Pinnick, E. R.; Erramilli, S.; Wang, F. *Mol. Phys.* **2010**, *108*, 2027−2036.
(57) Nakasako, M. *Phil. Trans. R. Soc. London B* **2004**, *359*, 1191−1206.
(58) Chakraborty, S.; Sinha, S. K.; Bandyopadhyay, S. *J. Phys. Chem. B* **2007**, *111*, 13626−13631.
(59) Stirnemann, G.; Castrillon, S. R. V.; Hynes, J. T.; Rossky, P. J.; Debenedetti, P. G.; Laage, D. *Phys. Chem. Chem. Phys.* **2011**, *13*, 19911−19917.
(60) Yokomizo, T.; Higo, J.; Nakasako, M. *Chem. Phys. Lett.* **2005**, *410*, 31−35.
(61) Thomas, A. S.; Elcock, A. H. *J. Am. Chem. Soc.* **2007**, *129*, 14887−14898.
(62) Leontidis, E.; Aroti, A.; Belloni, L.; Dubois, M.; Zemb, T. *Biophys. J.* **2007**, *93*, 1591−1607.
(63) Ninham, B. W.; Yaminsky, V. *Langmuir* **1997**, *13*, 2097−2108.
(64) Stirolo, A. *Adsorpt. Sci. Technol.* **2011**, *29*, 211−258.
(65) Hansen, Y.; Gekle, S.; Netz, R. R. *Phys. Rev. Lett.* **2013**, *111*, 118103.
(66) Korreman, S. S.; Posselt, D. *Eur. Biophys. J.* **2001**, *30*, 121−128.